# Anomalous magnetization cycle of $UFe_4Al_8$ single crystals: A Mössbauer effect study

João C. Waerenborgh and António P. Gonçalves
*Departamento Química, Instituto Tecnológico e Nuclear, P 2686-953 Sacavém, Portugal*

Grégoire Bonfait
*Departamento Química, Instituto Tecnológico e Nuclear, P 2686-953 Sacavém, Portugal*
*and Departamento Física, Faculdade de Ciências e Tecnologia, Universidade Nova de Lisboa, P 2825 Monte da Caparica, Portugal*

Margarida Godinho
*Departamento Física, Faculdade de Ciências da Universidade de Lisboa, P 1700 Lisboa, Portugal*

Manuel Almeida
*Departamento Química, Instituto Tecnológico e Nuclear, P 2686-953 Sacavém, Portugal*
(Received 6 April 1999)

An $^{57}$Fe Mössbauer spectroscopy study was performed on an $UFe_4Al_8$ single crystal, in an external magnetic field $\mathbf{B}_{ext}$, subtending an angle of 11° at the *b* axis. It shows that, even in low fields, the configuration of the Fe magnetic moments, $\mu_{Fe}$, is consistent with the canted antiferromagnetic order of $\mu_{Fe}$, established by single-crystal neutron diffraction in a field of 4.6 T. The canting of $\mu_{Fe}$ is always observed towards the direction of the U magnetic moments $\mu_U$, clearly showing that it is induced by $\mu_U$ rather than by $\mathbf{B}_{ext}$. At a certain value of $\mathbf{B}_{ext}$ during the magnetic domain rotation, the direction of $\mu_{Fe}$ is found to be temporarily frozen approximately along the direction of $\mathbf{B}_{ext}$. This confirms previous magnetization and magnetoresistance data, which show that for the same values of $\mathbf{B}_{ext}$, $\mu_U$ is blocked perpendicularly to $\mathbf{B}_{ext}$. Furthermore, the present study reveals that this blocking is a metastable state with a relaxation time of a few hours, at 4.2 K. [S0163-1829(99)03230-0]

## INTRODUCTION

$AFe_{12-x}X_x$ intermetallics ($A=f$ element, $X=p$ element), which crystallize in the $ThMn_{12}$-type structure, space group $I4/mmm$, may show relatively high Curie temperatures and considerable magnetic anisotropy as observed in $UFe_{10}Si_2$.[1] Phenomenological theories used to explain the magnetic behavior of these materials rely on an understanding of the interaction between the *f* element and the transition metal sublattices.[2] The study of $AFe_4Al_8$-ordered compounds, where the sublattices of Fe (magnetic) and Al (nonmagnetic) are clearly separated, is an important contribution to this goal.

In $UFe_4Al_8$ the U atoms occupy the $2a$ sites and ideally the $8f$ site is only occupied by Fe atoms, while the Al atoms occupy the $8j$ and $8i$ sites (Fig. 1). This compound shows a ferromagneticlike behavior below 150 K.[3] Extensive studies by means of magnetization measurements, Mössbauer spectroscopy, and neutron diffraction techniques on powder samples led to contradictory interpretations of the magnetic configuration of the Fe and U atoms.[4–9] These conflicting results may in part be explained by slight deviations from ideal stoichiometry as well as by a certain freedom of choice of site ($8f$-$8j$) by the Fe atom.[9] In the $UFe_xAl_{12-x}$ intermetallics, namely, in the case of $UFe_{5.8}Al_{6.2}$, the resulting structural disorder was found to be strongly dependent on the synthesis conditions.[10]

Large single crystals of $UFe_4Al_8$ (Ref. 11) have been recently prepared, and a systematic research program including magnetization, magnetoresistance, and neutron diffraction studies on the single-crystalline material was undertaken. Magnetization measurements confirmed a large magnetic anisotropy showing that *a* and *b* are equally easy axes.[12] Large magnetoresistance anomalies observed on these single crystals suggest that during a cycle the global magnetization **M** remains blocked perpendicularly to the external magnetic field $\mathbf{B}_{ext}$.[13] This interpretation is supported by the observation of steps in the magnetization curves measured both parallel and perpendicularly to $\mathbf{B}_{ext}$ and can only be understood if there is a large magnetic anisotropy within the basal plane.[13] In the $UFe_4Al_8$ system, where the U and Fe moments ($\mu_U$ and $\mu_{Fe}$, respectively) have different directions, a configuration in which the total moment can remain perpendicular to $\mathbf{B}_{ext}$ may be a consequence of the complex inter-

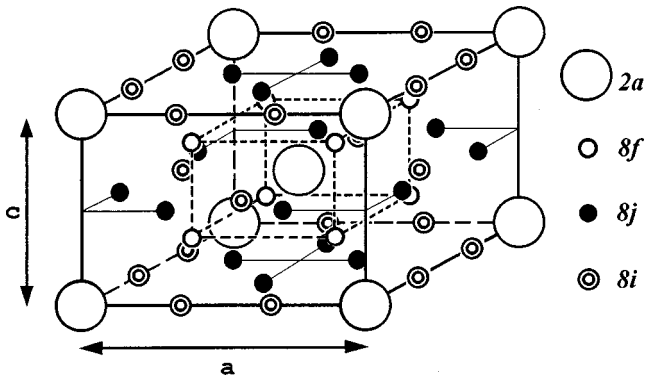


FIG. 1. Crystallographic unit cell of $UFe_4Al_8$ ($ThMn_{12}$-type structure). The U atoms are located at the origin and body-centered positions ($2a$ sites). The $8f$ sites are fully occupied by Fe and the $8j$ and $8i$ sites by Al.

 

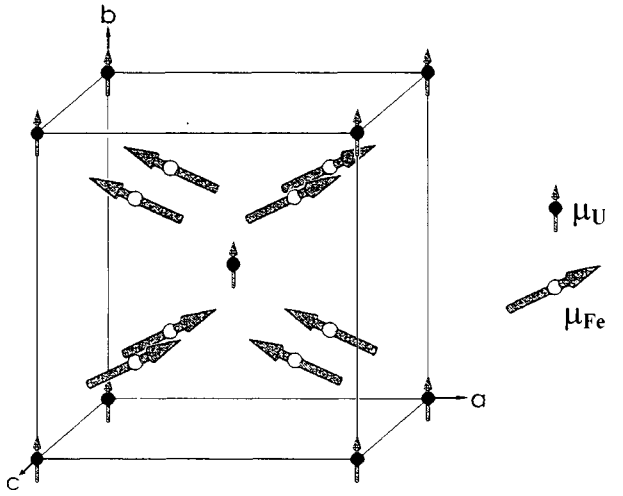


FIG. 2. Magnetic structure of $UFe_4Al_8$ in an applied field of 4.6 T (from Ref. 14). The solid points are the U atoms while the open points are the Fe atoms.

actions between the different $\mu_U$ and $\mu_{Fe}$.

Single-crystal neutron diffraction studies[14] have finally shown that in this compound, at 4.2 K, the Fe sublattice orders in a commensurate antiferromagnetic configuration with a moment of $\approx 1.1\mu_B$ per Fe atom, lying on the basal plane of the tetragonal structure. In a magnetic field of 4.6 T and by polarized neutrons, a ferromagnetic order of $\mu_U$ on the basal plane, with $\mu_U = 0.47\mu_B$, was deduced (Fig. 2). When the magnetic field was applied along the [010] direction, the antiferromagnetic $\mu_{Fe}$ were, as a first approximation, perpendicular to $\mathbf{B}_{ext}$, but showed a weak ferromagnetic component (Fig. 2). In combination with magnetization data, a canting of the Fe moments of 25° towards the $\mathbf{B}_{ext}$ direction was estimated for a 4.6 T field, and the remanence measured when $\mathbf{B}_{ext}$ was turned off indicated a canting of 16° of $\mu_{Fe}$ towards $\mu_U$ provided the U moment was still $0.47\mu_B$.

Neutron data, however, did not confirm the anomalous magnetization process detected by Bonfait *et al.*[13] Up to now, information on this process was only obtained from techniques which are sensitive to the bulk magnetization of $UFe_4Al_8$. New and valuable information can be obtained from $^{57}$Fe Mössbauer spectroscopy which only probes the Fe magnetic sublattice and therefore can give direct evidence on the rotation of the Fe moments, as long as the measurements are performed on a single crystal. Preliminary results showed that at a certain threshold value of $\mathbf{B}_{ext}$, when magnetic domains are rotating, an energy barrier on the easy magnetization direction perpendicular to $\mathbf{B}_{ext}$ was found.[15] A Mössbauer study of the full magnetization cycle is reported in this work.

## EXPERIMENT

A large single crystal with $UFe_4Al_8$ composition, grown by the Czochralski method as described in Ref. 11, was aligned in a CAD-4 diffractometer. The growth direction of the single crystal was found to subtend an angle of 11° at the crystallographic direction *b* and an angle of 79° at *a*, these three directions being approximately coplanar.

In order to prepare a single-crystalline disk with a suitable thickness for Mössbauer spectroscopy, a slice was cut out of the single crystal perpendicularly to the growth direction. The obtained disk (approximately 5 mm in diameter) was mounted on resin and polished until a thickness of 65 $\mu$m was achieved. The absorption coefficient of the 14.4 keV $\gamma$ radiation for $UFe_4Al_8$, estimated from the mass absorption coefficient of the elements,[16] is 18.5 mg/cm$^2$. For this absorption coefficient, according to the criteria of Long *et al.* for obtaining the best signal-to-noise ratio in Mössbauer spectra,[16] the optimal thickness of the single crystal should be $\approx 20$ $\mu$m. However, since cracks were starting to appear at the surface of the material, further thinning of the crystal was not performed in order to preserve the sample integrity. The 65-$\mu$m-thick disk was mounted on the Mössbauer cryostat in such a way that the $\gamma$-ray beam was perpendicular to the disk surface and therefore subtended an angle of 11° at the *b* axis, as shown in Fig. 3. $\mathbf{B}_{ext}$ was always applied parallel to the $\gamma$-ray beam direction.

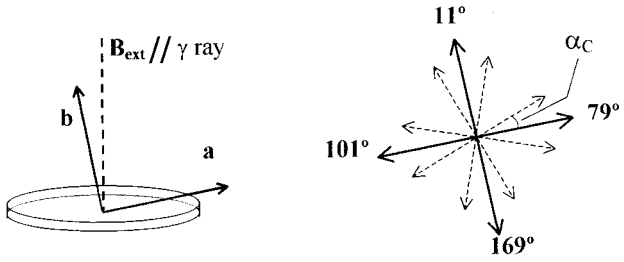


FIG. 3. Schematic representation of the alignment of the single crystalline absorber in the Mössbauer cryostat (for in-field Mössbauer measurements). Directions of $\mu_U$ (darker vectors) and $\mu_{Fe}$ (dashed vectors) for the four magnetic domains are shown on the right. $\alpha_C$ are the canting of $\mu_{Fe}$ towards $\mu_U$. $\mathbf{B}_{hf}$ are antiparallel to the corresponding $\mu_{Fe}$.

$^{57}$Fe Mössbauer spectra were collected at 297 and 4.2 K using a conventional spectrometer with a $^{57}$Co source in Rh matrix and a sinusoidal velocity vs time waveform. The spectrometer was calibrated against an $\alpha$-Fe foil. Spectra with the sample in an applied external magnetic field $\mathbf{B}_{ext}$ (up to 5 T) were obtained at 4.2 K, after zero-field cooling (ZFC), using a superconducting coil. The field at the source was less than 50 Oe. The sample was kept for $\approx 120$ h at each value of the applied $\mathbf{B}_{ext}$ in order to collect spectra with reasonable statistics. The spectra were fitted to Lorentzian lines using a nonlinear least-squares computer method.[17] The widths and areas of the peak pairs (1-6), (2-5), and (3-4) in each magnetic sextet were always kept equal during refinement. The fitting strategy for each spectrum is explained below.

The hysteresis curve of a single crystal of $UFe_4Al_8$ from the same batch of that used to prepare the Mössbauer absorber was obtained in a superconducting quantum interference device (SQUID) magnetometer. The orientation of this crystal relative to $\mathbf{B}_{ext}$ was similar to that used in the Mössbauer experiment. Magnetization measurements were performed at 4.2 K, after ZFC, with $\mathbf{B}_{ext}$ between $-3$ and 3 T.

## MAGNETIZATION CURVE

The hysteresis curve is shown in Fig. 4. In the range $1.5\,\mathrm{T} < \mathbf{B}_{ext} < 2.2\,\mathrm{T}$, where the domain rotation leads to a

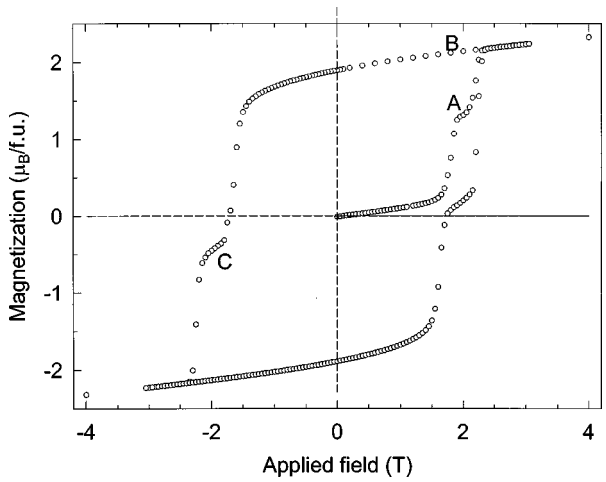


FIG. 4. Virgin magnetization and hysteresis curve of the $UFe_4Al_8$ single crystal at 4.2 K.

steep increase of the magnetization with $\mathbf{B}_{ext}$, the virgin magnetization curve is characterized by a step between 1.7 and 2.2 T (labeled *A* in Fig. 4) where the slope of the *M* vs $B_{ext}$ curve is very small. The magnetization value at this step, $M(A)$, is approximately half of the value $M(B)$ obtained for the same $\mathbf{B}_{ext}$ (label *B* in Fig. 4) after applying a field higher than 2.5 T, i.e., in a single magnetic domain state with all $\mu_U$ aligned along $\mathbf{B}_{ext}$. The word ''saturation'' will be used hereafter to designate this state although a slow increase of *M* with $B_{ext}$ is observed for $B_{ext} > 2.5$ T up to the highest measured field 5 T. This slow increase of *M* is interpreted as a progressive alignment of $\mu_{Fe}$ with $\mathbf{B}_{ext}$.

Considering the full hysteresis curve, another step (labeled *C* in Fig. 4) corresponding to a near-zero *M* value is observed. Both steps *A* and *C* are similar to those previously reported by Godinho *et al.*[12] and were explained by Bonfait *et al.*[13] as a blocking of the magnetization perpendicularly to $\mathbf{B}_{ext}$ that occurs during the rotation process of antiparallel domains towards the direction of $\mathbf{B}_{ext}$. Step *A*, on the virgin magnetization curve, corresponds to 50% of the domains aligned perpendicularly and the remaining 50% parallel to $\mathbf{B}_{ext}$, while step *C* corresponds to 100% of the domains aligned perpendicularly to $\mathbf{B}_{ext}$.[13] In contrast to what is observed at 4.2 K, the virgin magnetization curve obtained at 2 K (Ref. 13) shows an additional first step at 1/4 of $M(B)$, corresponding to only 25% of the domains aligned parallel to $\mathbf{B}_{ext}$, also explained by the same blocking magnetization phenomena. At 4.2 K this step is not visible probably because it occurs in a very narrow range of $\mathbf{B}_{ext}$ values and due to relaxation phenomena.

## MÖSSBAUER MEASUREMENTS

The Mössbauer spectrum of the single-crystalline $UFe_4Al_8$ disk taken at room temperature show an asymmetric quadrupole doublet with isomer shift $\delta$ and quadrupole splitting $\Delta$ (Table I) equal to those observed in powder $UFe_4Al_8$ samples.[9] The point symmetry of the $8f$ site is $2/m$, which means that the electric field gradient is not axially symmetric (the main symmetry axis should be at least threefold). In this case information from the relative areas of the doublet peaks can only be obtained if the asymmetry parameter of the electric field gradient and both the polar and azimuthal angles of the $\gamma$-ray direction referred to the electric field gradient axes system were known.[18] An analysis of the electric charge distribution around the $8f$ site is beyond the scope of this paper.

A first set of Mössbauer spectra with the absorber at 4.2 K and in different fields was performed. For $\mathbf{B}_{ext}=0$, after ZFC, the spectrum (Fig. 5), hereafter referred to as $s(1;0\ \mathrm{T})$, may be fitted by a sextet with hyperfine parameters: $\delta$, quadrupole shift $\varepsilon$, and hyperfine field $B_{hf}$ (Table I), in good agreement with powder Mössbauer data.[9]

The spectrum obtained with $\mathbf{B}_{ext}=1.5$ T (Fig. 5) was analyzed assuming that the magnetic structure type deduced from neutron diffraction at 4.6 T is also valid for $\mathbf{B}_{ext}=1.5$ T, probably with a smaller canting angle for $\mu_{Fe}$. After ZFC there are four possible magnetic domain directions determined by the alignment of $\mu_U$ along both directions of the *a* and *b* axes. As referred to above, the single-crystalline absorber was mounted in the Mössbauer cryostat in such a way that the *b* and *a* axes subtended angles of 11° and 79°, respectively, at the direction of $\mathbf{B}_{ext}$. The four magnetic domains can be identified by the angles between $\mu_U$ and $\mathbf{B}_{ext}$: $\theta_U=11°$, 79°, 101°, and 169° (Fig. 3 and Table II). Considering a nonzero canting, eight $\mu_{Fe}$ directions correspond to this configuration. The angles $\theta_{Fe}$ between these directions and $\mathbf{B}_{ext}$ as well as the angles $\theta$ subtended by the $\mathbf{B}_{hf}$ at $\mathbf{B}_{ext}$ are given in Table II. Since each $\mathbf{B}_{hf}$ is antiparallel to the corresponding $\mu_{Fe}$,[18] all the $\theta=\theta_{Fe}-180°$.

When $B_{ext}$ is switched on, as long as there are four magnetic domains, eight magnetic sextets corresponding to eight effective fields at the Fe nuclei given by

$$B_{eff}(\theta)=\sqrt{B_{ext}^2+B_{hf}^2+2B_{hf}B_{ext}\cos\theta} \qquad (1)$$

are expected.

The relative intensities of peak pairs (1,6), (2,5), and (3,4) for each sextet, $I_{1,6}$, $I_{2,5}$, and $I_{3,4}$, respectively, are determined by the angle $\xi$ between $\mathbf{B}_{eff}$ and the Mössbauer $\gamma$ rays, i.e., the direction of $\mathbf{B}_{ext}$. In an absorber with ideal thickness, $I_{1,6}$, $I_{2,5}$, and $I_{3,4}$ are equal to[18]

$$3:\frac{4\sin^2\xi}{1+\cos^2\xi}:1 \quad \text{with} \quad \cos\xi=\frac{B_{hf}\cos\theta+B_{ext}}{B_{hf}}. \qquad (2)$$

For a single-crystalline $UFe_4Al_8$ disk with a thickness of $\approx 65$ $\mu$m, the usual dimensionless thickness parameter $t_A$, given by

$$t_A=n_{Fe}f_A\sigma_0,$$

is $\approx 6.6 f_A$, where $f_A$ is the recoilless fraction, $\sigma_0=2.6\times10^{-18}\ \mathrm{cm}^2$ the cross section at resonance for the $^{57}$Fe 14.4 keV Mössbauer transition,[18] and $n_{Fe}$ the number of $^{57}$Fe atoms per cm$^2$ in the absorber. For this absorber the resonant absorption area is not concentrated under a single peak, but is spread over several peaks, at least six being always resolved in the Mössbauer spectra (Fig. 5). Nevertheless, for $f_A \approx 1$, $t_A$ is still high and a linear dependence between the area of a peak and the $n_{Fe}$ contributing to that peak should not be expected. The higher $n_{Fe}$, the more reduced is the peak area relative to the value it should have if a linear dependence is assumed,[18] i.e., relative to the values obtained from Eq. (2).

TABLE I. Estimated parameters from the Mössbauer spectra taken at 4.2 K (except otherwise stated) and in a magnetic field $\mathbf{B}_{ext}$. $\delta$ isomer shift relative to metallic Fe at 297 K. $\Delta$ quadrupole splitting and $\varepsilon$ quadrupole shift measured in the paramagnetic and magnetically ordered state, respectively. $B_{eff}$ effective field at the Fe nuclei; $I_{1,6}$ and $I_{2,5}$ areas of peak pairs (1,6) and (2,5) relative to $I_{3,4}$ of each sextet; $I$ relative area of each sextet; $\theta$ angle between $\mathbf{B}_{ext}$ and $\mathbf{B}_{hf}$, $\theta_U$ angle between $\mathbf{B}_{ext}$ and $\mu_U$; $\alpha_C$ canting angle of $\mu_{Fe}$. The estimated standard deviations are $\leq$0.02 mm/s for $\delta$, $\varepsilon$, and $\Delta$, $\leq$0.2 for $I_{n,m}$, $\leq$2% for $I$, and $\leq$0.1 T for the refined $B_{eff}$.

| $\mathbf{B}_{ext}$ | $\delta$ | $\Delta$, $\varepsilon$ | $\mathbf{B}_{eff}$ | $I_{1,6}$ | $I_{2,5}$ | $I$ | $\theta$[a] | $\alpha_C$ | $\theta_U$[a] |
|---|---|---|---|---|---|---|---|---|---|
| 0 T (297 K) | 0.16 | 0.33 | | | | 100% | | | |
| 0 T | 0.28 | 0.12 | 11.0 | 2.5 | 0.8 | 100% | | | |
| 1.5 T | 0.28 | 0.11 | 10.9 | 2.6 | 3.4 | 11% | 97°±5° | 18°±5° | 11° |
| | | | 10.5 | 2.6 | 2.8 | 11% | 114°±5° | 13°±5° | |
| | | 0.13 | 12.4 | 2.6 | 0.4 | 17% | <35° | | 79° |
| | | | 9.6 | 2.6 | 0.1 | 17% | >156° | | |
| | | 0.13 | 12.5 | 2.6 | 0.02 | 12% | <27° | | 101° |
| | | | 9.7 | 2.6 | 0.6 | 12% | >149° | | |
| | | 0.11 | 11.8 | 2.7 | 2.1 | 10% | 61°±7° | 18°±7° | 169° |
| | | | 11.4 | 2.7 | 3.0 | 10% | 78°±6° | 23°±6° | |
| 2 T | 0.28 | 0.10 | 10.9 | 2.4 | 1.6 | 50% | 98°±5° | 19°±5° | 11° |
| | | 0.13 | 10.0 | 2.4 | 1.5 | 50% | 125°±5° | 24°±5° | |
| 5 T | 0.29 | 0.12 | 10.2 | 2.4 | 3.2 | 50% | 112°±1° | 33°±1° | 11° |
| | | 0.12 | 8.4 | 2.4 | 1.2 | 50% | 133°±1° | 32°±1° | |
| 1.5 T (2 T)[b] | 0.29 | 0.12 | 10.9 | 2.6 | 3.2 | 30% | 97°±5° | 18°±5° | 11° |
| | | | 10.4 | 2.6 | 2.6 | 30% | 117°±5° | 16°±5° | |
| | | | 12.4[c] | 2.6 | 0.4 | 20% | <35° | | 79° |
| | | | 9.6[c] | 2.6 | 0.2 | 20% | >156° | | |
| −1.5 T | 0.28 | 0.12 | 12.4[c] | 2.7 | 0.4 | 7% | <35° | | 79° |
| | | | 9.6[c] | 2.7 | 0.1 | 7% | >156° | | |
| | | 0.12 | 12.5[c] | 2.6 | 0.02 | 17% | <27° | | 101° |
| | | | 9.7[c] | 2.6 | 0.6 | 17% | >149° | | |
| | | 0.12 | 11.8 | 2.6 | 2.4 | 26% | 61°±7° | 18°±7° | 169° |
| | | | 11.4 | 2.6 | 3.4 | 26% | 78°±6° | 23°±6° | |
| −2 T | 0.28 | 0.12 | 11.0 | 2.7 | 1.5 | 50% | 95°±5° | 16°±5° | 11° |
| | | | 9.9 | 2.7 | 1.5 | 50% | 128°±5° | 27°±5° | |

[a] $\theta$ and $\theta_U$ are always defined relative to the $B_{ext}$. When $B_{ext}$ is negative the polar directions defined by $\theta$ and $\theta_U$ are also reversed in the coordinate system associated with the crystal axes.

[b] Spectrum taken in $B_{ext}=1.5$ T after applying a field of 2 T to the sample, for 10 min.

[c] Values kept constant during refinement.

The spectrum $s(1;1.5\,\mathrm{T})$ was therefore fitted taking as starting values of the hyperfine parameters the set of eight $B_{eff}$ given by Eq. (1) with $B_{ext}=1.5$ T, $B_{hf}=11$ T, $\theta$ taken from Table II assuming the canting angle $\alpha_C=16°$,[14] and $I_{2,5}$ given by Eq. (2). The $I_{2,5}$ had to be kept constant during refinement; $I_{1,6}$, $\delta$, and the quadrupole shifts $\varepsilon$ were refined, but assumed equal for all sextets; $B_{eff}$ and relative areas $I$ were allowed to vary. The pair of $I$ values corresponding to the Fe atoms antiferromagnetically coupled to the same $\mu_U$ direction were kept equal. In a second stage of refinement the $I_{2,5}$ were recalculated in agreement with the new estimated $B_{eff}$ values. After three or four stages of refinement, the $B_{eff}$ values did not vary significantly. Due to saturation effects, the estimated values for the $I_{1,6}$ are 2.6 (Table I), lower than the theoretical value 3. Values of $I_{2,5}$ lower than those estimated from Eq. (2) were therefore introduced in the final stages of refinement, improving the quality of the fit. These values take into account that the saturation effects are more important the higher the $n_{Fe}$ contributing to the Mössbauer peak, as referred to above. The ratios between the observed and theoretical values of $I_{2,5}$ are thus >2.6/3 if the $I_{2,5}$ calculated from Eq. (2) are >3, ≈2.6/3 if they are ≈3, and <2.6/3 if they are <3. In the final results (Table I) and considering the experimental errors, the corrected $I_{2,5}$ were found to be consistent with the corresponding values estimated for the $B_{eff}$.

It should be noted that the difference between the estimated $B_{eff}$ for the Fe atoms coupled to $\mu_U$ with $\theta_U=79°$ and 101° is ≈0.1 T, similar to the estimated error for the $B_{eff}$ ($\leq$0.1 T). This is not the case for the other $B_{eff}$. Therefore, while all the sextets associated with $\mu_{Fe}$ approximately perpendicular to $\mathbf{B}_{ext}$ (i.e., coupled to $\mu_U$ with $\theta_U=11°$ and 169°) are clearly distinguished from the other sextets, those associated with $\mu_{Fe}$ approximately parallel to $\mathbf{B}_{ext}$ (i.e., coupled to $\mu_U$ with $\theta_U=79°$ and 101°) are not distinguished from each other by the Mössbauer data. Nevertheless, the latter four sextets were kept in the final adjustment since they produce a better fitting than the analysis where their contribution was reduced to only two subspectra.

From the analysis of $s(1;1.5\,\mathrm{T})$ it can be concluded that ≈42% of the $\mu_U$ are aligned along the $b$ axis (≈22% parallel and ≈20% antiparallel to $b$) and ≈58% of the $\mu_U$ are aligned

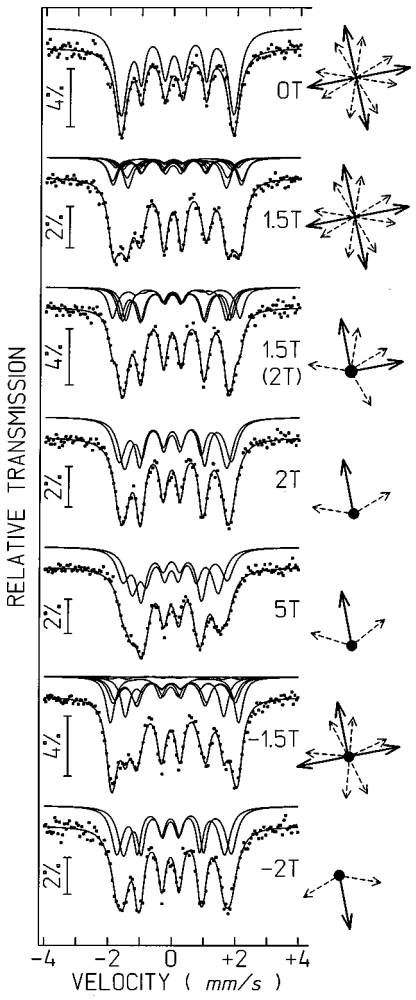


FIG. 5. Mössbauer spectra of the $UFe_4Al_8$ single crystal taken at 4.2 K after ZFC in zero field and in applied magnetic fields of 1.5 T, $s(1;1.5\,T)$; 1.5 T after being submitted to 2 T for 10 min, $s(2;2\,T,1.5\,T)$; 2 T, $s(2;2\,T)$; 5 T, $s(2;5\,T)$; $-1.5$ T, $s(2;5\,T,-1.5\,T)$, and $-2$ T, $s(2;5\,T,-2\,T)$. The calculated function is plotted on the experimental points. Calculated magnetic sextets corresponding to the different $B_{eff}$ values are also plotted slightly shifted. On the right-hand side are shown the directions of $\mu_U$ and $\mu_{Fe}$ (see Fig. 3) deduced from the analysis of each spectrum.

along *a*, but the data are not accurate enough to distinguish between those which are parallel and those which are antiparallel to *a*. From the $B_{eff}$ values corresponding to $\theta = 101° \pm \alpha_C$ and $79° \pm \alpha_C$, an average value $\alpha_C \approx 18(7)°$ may also be deduced. No reliable estimate of $\alpha_C$ can be given based on the remaining four values of $B_{eff}$ due to the $B_{eff}$ cosine type of dependence on $\theta$ [Eq. 1]: when $\theta \leqslant 30°$ or $\theta \geqslant 150°$, uncertainties of 0.1 T in $B_{eff}$ are reflected in uncertainties of $\approx 25°$ in $\theta$ and, consequently, on $\alpha_C$. Considering the experimental uncertainties, $\alpha_C \approx 18(7)°$ is in good agreement with the values of the canting angle deduced from neutron diffraction for $B_{ext} = 4.6$ T (25.4°) and from the remanent magnetization, 16°.[14] The $\alpha_C$ estimated from $s(1;1.5\,T)$ for both magnetic domains defined by $\theta_U = 11°$ and $\theta_U = 169°$ indicates that $\mu_{Fe}$ are canted towards $\mu_U$ to which they are coupled. In the $\theta_U = 169°$ case $\mu_U$ are almost antiparallel to $\mathbf{B}_{ext}$. Therefore, while neutron data could only deduce a canting of $\mu_{Fe}$ towards $\mathbf{B}_{ext}$, the analysis of $s(1;1.5\,T)$ clearly shows that the canting of $\mu_{Fe}$ is induced by $\mu_U$ and not by $\mathbf{B}_{ext}$.

TABLE II. Angles $\theta_U$, $\theta_{Fe}$, and $\theta$ subtended by $\mathbf{B}_{ext}$ at $\mu_U$, $\mu_{Fe}$, and $\mathbf{B}_{hf}$, respectively. $\alpha_C$ is the canting angle of $\mu_{Fe}$.

| $\theta_U$ | $\theta_{Fe}$ | $\theta$ |
|---|---|---|
| 11° | $101° - \alpha_C$ | $79° + \alpha_C$ |
| | $79° - \alpha_C$ | $101° + \alpha_C$ |
| 79° | $11° - \alpha_C$ | $169° + \alpha_C$ |
| | $169° - \alpha_C$ | $11° + \alpha_C$ |
| 101° | $11° + \alpha_C$ | $169° - \alpha_C$ |
| | $169° + \alpha_C$ | $11° - \alpha_C$ |
| 169° | $101° + \alpha_C$ | $79° - \alpha_C$ |
| | $79° + \alpha_C$ | $101° - \alpha_C$ |

The magnetic field was further increased up to 2 T, the value corresponding to the step labeled *C* on the virgin magnetization curve (Fig. 4). In the spectrum obtained at 2 T, $s(1;2\,T)$, Fig. 5, the largest $B_{eff}$ that may be fitted is $\leqslant 11$ T. If some $\mu_U$ were still parallel to *a*, i.e., blocked perpendicularly to $\mathbf{B}_{ext}$, $B_{eff}$ corresponding to $\theta$ in the range 0°–11°, and consequently larger than 12.5 T, should have been observed. In fact, the spectrum is satisfactorily fitted assuming only two values of $B_{eff}$ (Table I) corresponding to $\theta \approx 98°$ and $\approx 125°$, i.e., consistent with all $\mu_U$ subtending an angle of 11° at $\mathbf{B}_{ext}$ and an average $\alpha_C = 22(5)°$. The average $\alpha_C$ value is slightly larger than that measured when $\mathbf{B}_{ext} = 1.5$ T, however, considering the experimental errors this difference is probably not significant.

The agreement between the experimental points on the Mössbauer spectra and the calculated functions based on the magnetic structure deduced from neutron data is good, as may be seen in Fig. 5. At first sight, the fact that the zero-field-cooled sample has reached saturation when $B_{ext} = 2$ T seems to be contradictory with the virgin magnetization curve (Fig. 4). However, in order to obtain a Mössbauer spectrum, the crystal is subjected to $\mathbf{B}_{ext}$ during a much longer time ($\approx 120$ h) than in the case of the magnetization measurements performed in a SQUID (a few minutes). Under these circumstances and if the domain rotation is a thermally activated process with a relaxation time at 4.2 K of a few hours, the blocking of **M** perpendicularly to $\mathbf{B}_{ext}$ might have passed unnoticed by the Mössbauer effect. A thermal-activated process is consistent with the fact that, as the temperature at which the hysteresis curves are measured increases, the slopes of *M* vs $B_{ext}$ observed on the steps of these curves become larger.[12,13] Furthermore, such a relaxation process can also explain why the virgin magnetization curve obtained at 4.2 K shows only one step, whereas at 2 K two steps are visible.[13]

Since it is not possible to obtain a reliable Mössbauer spectrum in a time much shorter than 1 day, the magnetic domain configuration obtained during step *A* (Fig. 4) was ''quenched'' by the following process. The sample was first allowed to warm up to room temperature (well above $T_{ord}$ of $UFe_4Al_8$) and then cooled down again to 4.2 K in order to ensure that the crystal had no memory from previous magnetization processes. Spectrum $s(2;1.5\,T)$, the first of the second set of Mössbauer spectra, was taken and found to be similar to $s(1;1.5\,T)$, thus confirming the virgin state of the

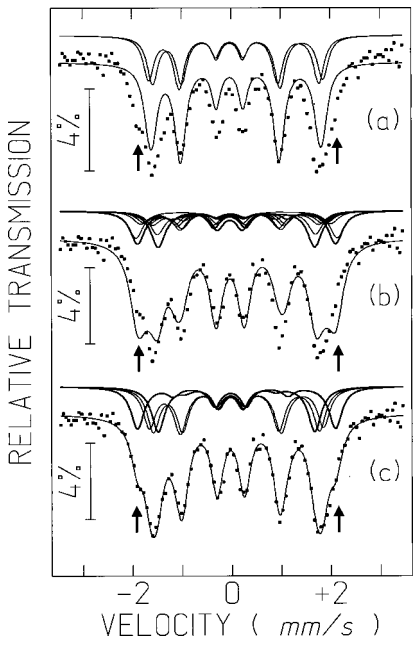


FIG. 6. Mössbauer spectrum $s(2;2\ \mathrm{T},1.5\ \mathrm{T})$ of the zero-field-cooled $UFe_4Al_8$ single crystal taken at 4.2 K and in an external field of 1.5 T after being submitted to an external field of 2 T for 10 min. The calculated functions plotted on the experimental points correspond to (a) the simulated function assuming that all $\mu_U$ are parallel to the *b* axis. (b) The simulated function assuming the magnetic domain configuration deduced from spectrum $s(1;1.5\ \mathrm{T})$ (Fig. 5). (c) The function fitted to the spectrum. Arrows mark the Dopler velocity ranges where differences in the relative absorption of the three calculated functions are more conspicuous.

crystal. The zero-field-cooled crystal was then submitted to $B_{ext}=2$ T for a short time, 10 min, and then brought back to $B_{ext}=1.5$ T in order to avoid relaxation towards the saturated state. The spectrum $s(2;2\ \mathrm{T},1.5\ \mathrm{T})$ was accumulated at this state (Figs. 5 and 6). The field 1.5 T was expected to be too weak to force the rotation of the magnetic moments towards the easy magnetization direction closer to the direction of $\mathbf{B}_{ext}$, but hopefully strong enough to keep the magnetic domain configuration achieved while the sample was subjected to 2 T.

The spectrum $s(2;2\ \mathrm{T},1.5\ \mathrm{T})$ is compared to the spectrum simulated assuming that all $\mu_U$ were parallel to $\mathbf{B}_{ext}$ [Fig. 6(a)] and to the spectrum calculated for $s(1;1.5\ \mathrm{T})$ [Fig. 6(b)]. These figures clearly show that a different magnetic configuration was achieved by the above described ''quenching'' process.

In the simulated spectrum in Fig. 6(a), only the magnetic sextets corresponding to $B_{eff}=10.9$ and 10.5 T are present. Differences between the simulated spectrum and $s(2;2\ \mathrm{T},1.5\ \mathrm{T})$ are particularly evident at the outer limits of the spectrum envelope, marked by arrows in Fig. 6(a), clearly showing that in order to fit $s(2;2\ \mathrm{T},1.5\ \mathrm{T})$, two more sextets, $B_{eff}=12.4$ and 9.7 T [bold in Figs. 6(b) and 6(c)], corresponding to either $\theta\approx 101°\pm\alpha_C$ or $\theta\approx 79°\pm\alpha_C$, have to be considered.

On the other hand, spectra $s(1;1.5\ \mathrm{T})$ and $s(2;2\ \mathrm{T},1.5\ \mathrm{T})$ are also different [Fig. 6(b)]. In particular, the relative intensities of the lowest- and highest-velocity peaks observed in the spectrum $s(1;1.5\ \mathrm{T})$, marked by arrows in Figs. 6(b) and 6(c), are higher than in $s(2;2\ \mathrm{T},1.5\ \mathrm{T})$ where these peaks are actually reduced to shoulders at the lowest- and highest-velocity limits of the spectrum.

Starting the analysis of $s(2;2\ \mathrm{T},1.5\ \mathrm{T})$ with the magnetic sextets fitted to $s(1;1.5\ \mathrm{T})$ (Table I) and keeping constant the values of the $B_{eff}=12.4$, 9.6, 12.5, and 9.7 T, the fitting procedure shows that this change in shape is accommodated by reducing to vanishingly small values the relative areas of the sextets $B_{eff}=12.5$, 9.7, 11.8, and 11.4 T. The suppression of the magnetic sextets with larger $B_{eff}$ is obviously necessary to accommodate the observed decreasing in relative intensity of the outer limits of $s(2;2\ \mathrm{T},1.5\ \mathrm{T})$; the elimination of the 9.7 T sextet is not so obvious from the shape of the spectrum, but it is not surprising since the corresponding $\mu_{Fe}$ are antiferromagnetically coupled to those associated with the 12.5 T magnetic sextet. The last stage of refinement was therefore performed neglecting these four subspectra and the spectrum was perfectly explained by four magnetic sextets with the estimated parameters summarized in Table I. These data show that 40% of $\mu_{Fe}$ are coupled to $\mu_U$ aligned with *a* and 60% to $\mu_U$ parallel to *b*, the canting angle of $\mu_{Fe}$ being $\alpha_C=17(5)°$ similar to the $\alpha_C$ estimated for $s(1;1.5\ \mathrm{T})$.

As explained above, it is not possible to determine from the Mössbauer data if the $\mu_U$ aligned with *a* are associated with either $\theta_U=79°$ or 101°, due to the similarity of the corresponding $B_{eff}$ values. It is, however, possible to ascertain that the ≈60% of $\mu_U$ aligned with *b* are parallel to this axis. As the remaining 40% are perpendicular to it, the *M* value measured along $\mathbf{B}_{ext}$ should be approximately 60% of the saturation value. According to the hysteresis curve, $M(A)$ is ≈50% of the saturation value (Fig. 4). The agreement between the Mössbauer and magnetization data is satisfactory considering the experimental uncertainties. When a field of 2 T is applied for 10 min, roughly the time taken by a SQUID measurement of the *M* in the $B_{ext}$ range between 1.5 and 2 T, rotation of the whole antiparallel domain is observed. However, this rotation stops before $\mu_U$ are aligned along $\mathbf{B}_{ext}$; it stops when $\mu_U$ are aligned along a perpendicular direction in agreement with the blocking of **M** perpendicular to the direction of the field observed in the virgin magnetization curve for $B_{ext}=2$ T.

Increasing $B_{ext}$ again up to 2 T, a spectrum $s(2;2\ \mathrm{T})$ similar to $s(1;2\ \mathrm{T})$ was obtained, indicating that saturation was again reached when 2 T was applied during the time necessary to collect a Mössbauer spectrum. $\mathbf{B}_{ext}$ was increased up to 5 T, and the spectrum $s(2;5\ \mathrm{T})$ was taken, confirming that all $\mu_U$ were parallel to *b*. The estimated $\alpha_C=33°\pm1°$ is significantly higher than the $\alpha_C$ estimated from the spectra obtained with $\mathbf{B}_{ext}\leqslant 2$ T. Although the driving force for $\mu_{Fe}$ canting is $\mu_U$, as deduced from $s(1;1.5\ \mathrm{T})$, when the sample is saturated and all $\mu_U$ are aligned along the easy axis whose direction is closer to the $\mathbf{B}_{ext}$ direction, the canting angle becomes larger, in full agreement with the increase of *M* with $B_{ext}$ after saturation (Fig. 4).

After saturation at 5 T, the field was reversed and brought down to −1.5 T. The spectrum $s(2;5\ \mathrm{T},-1.5\ \mathrm{T})$ was accumulated while the field was kept at −1.5 T (Figs. 5 and 7). Differences in the relative intensities of the peaks at the lowest- and highest-velocity limits of $s(2;5\ \mathrm{T},-1.5\ \mathrm{T})$ as compared to $s(1;1.5\ \mathrm{T})$ and $s(2;2\ \mathrm{T},1.5\ \mathrm{T})$ are apparent (cf.

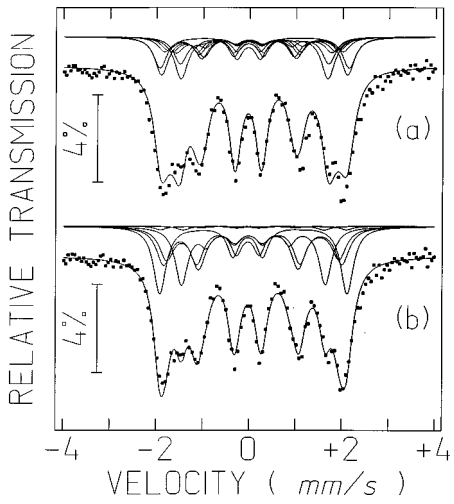


FIG. 7. Mössbauer spectrum $s(2;5\,\mathrm{T},-1.5\,\mathrm{T})$ of the $UFe_4Al_8$ single crystal after saturation, taken at 4.2 K, and in a reverse external field of −1.5 T. The calculated functions plotted on the experimental points correspond to (a) the simulated function assuming the magnetic domain configuration deduced from spectrum $s(1;1.5\,\mathrm{T})$ (Fig. 5) and (b) the function fitted to the spectrum.

Fig. 5 and 7). In Fig. 7(a) the spectrum calculated for $s(1;1.5\,\mathrm{T})$ is superimposed on the experimental points of $s(2;5\,\mathrm{T},-1.5\,\mathrm{T})$ in order to emphasize their differences. While in $s(1;2\,\mathrm{T},1.5\,\mathrm{T})$ the differences in shape relative to $s(1;1.5\,\mathrm{T})$ were accommodated by the elimination of two sextet pairs, $B_{\mathrm{eff}}=12.5$, 9.7 T and 11.8, 11.4 T (corresponding to $\theta_U=101°$ and $\theta_U=169°$), according to the analysis of $s(2;5\,\mathrm{T},-1.5\,\mathrm{T})$, only one of the sextet pairs, $B_{\mathrm{eff}}=10.9$, 10.4 T corresponding to $\theta_U=11°$, is virtually absent indicating that no $\mu_U$ are yet aligned along the new $\mathbf{B}_{\mathrm{ext}}$ direction as expected from magnetization data (Fig. 4). However, the relative area estimated for both sextets of the pair $B_{\mathrm{eff}}=11.8, 11.4\,\mathrm{T}$ amounts to only 50%, indicating that only ≈50% of $\mu_U$ remained frozen along the direction antiparallel to $\mathbf{B}_{\mathrm{ext}}$ ($\theta_U=169°$) and a large number, ≈50%, of $\mu_U$ rotated 90°, giving rise to domains where $\mu_U$ is aligned with *a*. This observation is at variance with the magnetization cycle (Fig. 4) according to which all $\mu_U$ remain aligned with the previous direction of saturation down to $\mathbf{B}_{\mathrm{ext}}\approx-1.5\,\mathrm{T}$.

As in the case of the $s(1;2\,\mathrm{T})$ spectrum, slow relaxation phenomena can explain these results. Also after ZEC one would expect that the four possible magnetic domains are equally probable; nevertheless, $s(1;1.5\,\mathrm{T})$ showed that the fraction of the domains with $\mu_U$ parallel to *a* is higher than that of the domains with $\mu_U$ parallel to *b*. A slow evolution of the magnetic system towards the configuration corresponding to step *A* while spectrum $s(1;1.5\,\mathrm{T})$ was accumulating and to step *C* in the case of $s(2;5\,\mathrm{T},-1.5\,\mathrm{T})$ would explain both data sets. Slightly above 1.5 T the rotation of the magnetic domains aligned antiparallel to $\mathbf{B}_{\mathrm{ext}}$, towards a direction perpendicular to $\mathbf{B}_{\mathrm{ext}}$, is observed in the hysteresis curve (Fig. 4). Keeping the system for 50 h in a field lower than, but close to, that critical value may allow the detection of the same effect, although at a slower rate. It should also be stressed that, instead of relaxing towards an alignment of the **M** along $\mathbf{B}_{\mathrm{ext}}$, both $s(1;1.5\,\mathrm{T})$ and $s(2;5\,\mathrm{T},-1.5\,\mathrm{T})$ spectra clearly show again that part of the magnetization is frozen in a perpendicular direction.

Finally, applying $B_{\mathrm{ext}}=-2\,\mathrm{T}$, the spectrum $s(2;-2\,\mathrm{T})$ similar to $s(1;2\,\mathrm{T})$ and $s(2;2\,\mathrm{T})$ is obtained, confirming that, as expected from the hysteresis curve (Fig. 4) and a thermally activated rotation process with a relaxation time of a few hours at 4.2 K, all the magnetic domains have rotated towards the new $\mathbf{B}_{\mathrm{ext}}$ direction and saturation was reached.

## CONCLUSION

The directions of $\mu_{\mathrm{Fe}}$ deduced from the Mössbauer spectra obtained for different $\mathbf{B}_{\mathrm{ext}}$ are consistent with an antiferromagnetic coupling of $\mu_{\mathrm{Fe}}$ which are approximately perpendicular to $\mu_U$, but with a large canting angle towards the $\mu_U$ direction. Mössbauer data therefore confirm that the magnetic structure determined by single-crystal neutron data in an external field $\mathbf{B}_{\mathrm{ext}}=4.6\,\mathrm{T}$ is also valid for lower fields, at least down to 1.5 T. In this field at 4.2 K, eight $\mu_{\mathrm{Fe}}$ directions corresponding to four magnetic domain directions (magnetization along both directions of *a* and *b*) are observed. For $\mathbf{B}_{\mathrm{ext}}\geqslant 2\,\mathrm{T}$ the magnetic domain configuration changes and $\mu_{\mathrm{Fe}}$ coupled to $\mu_U$ which are not favorably oriented relative to $\mathbf{B}_{\mathrm{ext}}$ rotate. The final directions of $\mu_{\mathrm{Fe}}$ are consistent with all $\mu_U$ being parallel to the easy magnetization direction which is nearest to the $\mathbf{B}_{\mathrm{ext}}$ direction.

The canting of $\mu_{\mathrm{Fe}}\approx 18°\pm 5°$ for $\mathbf{B}_{\mathrm{ext}}=1.5\,\mathrm{T}$ agrees with previous neutron diffraction results. Since for this field the zero-field-cooled crystal still has four magnetic domains and $\mu_{\mathrm{Fe}}$ always turn towards the $\mu_U$ direction even if it is antiparallel to $\mathbf{B}_{\mathrm{ext}}$, the present data further show that the driving force for the canting is induced by $\mu_U$. When the crystal is saturated, all the $\mu_U$ directions are parallel to the easy magnetization direction closer to the direction of $\mathbf{B}_{\mathrm{ext}}$ and the canting is found to increase with $B_{\mathrm{ext}}$ from about $22°\pm 5°$ at 2 T up to $33°\pm 2°$ at 5 T, in agreement with the increase of *M* with $B_{\mathrm{ext}}$ after saturation is reached (Fig. 4).

The most remarkable result is, however, the direct observation of the blocking of $\mu_{\mathrm{Fe}}$ along a direction close to the applied field direction at a certain threshold value of $B_{\mathrm{ext}}$ ($1.5\,\mathrm{T}<B_{\mathrm{ext}}<2\,\mathrm{T}$ at 4.2 K) during the magnetic domains rotation. Blocked $\mu_{\mathrm{Fe}}$ are coupled to $\mu_U$ aligned along the easy magnetization direction perpendicular to $\mathbf{B}_{\mathrm{ext}}$, in agreement with magnetization and magnetoresistance data,[13] which showed a blocking of the magnetization perpendicularly to the applied field at the same value of $B_{\mathrm{ext}}$.

Due to the different time scales of SQUID and Mössbauer measurements, the comparison between the results obtained by both techniques puts into evidence that the blocking of **M** perpendicular to $\mathbf{B}_{\mathrm{ext}}$ is a metastable state. A quenching procedure had to be used in order to probe this state by the Mössbauer effect. From the present data it is deduced that the rotation of magnetic domains aligned perpendicular to $\mathbf{B}_{\mathrm{ext}}$ is only severely hindered as compared to those which are antiparallel to $\mathbf{B}_{\mathrm{ext}}$. Given a long enough time, all the magnetic domains reach the easy magnetization axis most favorably aligned relative to the $\mathbf{B}_{\mathrm{ext}}$ direction. At the appropriate field value, approximately the middle value of step *A* in the *M* vs $B_{\mathrm{ext}}$ curve (Fig. 4), the relaxation time at 4.2 K is of the order of a few hours.

## ACKNOWLEDGMENT

This work was supported by PRAXIS (Portugal) under Contract No. PRAXIS/P/FIS/10040/1998.

[1] P. Estrela, M. Godinho, A. P. Gonçalves, M. Almeida, and J. C. Spirlet, J. Alloys Compd. **230**, 35 (1995).
[2] K. H. J. Buschow, J. Appl. Phys. **63**, 3130 (1988).
[3] A. Baran, W. Suski, and T. Mydlarz, J. Less-Common Met. **96**, 269 (1984).
[4] H. Ptasiewicz-Bak, A. Baran, W. Suski, and J. Leciejewicz, J. Magn. Magn. Mater. **76-77**, 439 (1988).
[5] W. Schäfer, G. Will, J. Gal, and W. Suski, J. Less-Common Met. **149**, 237 (1989).
[6] J. Gal, I. Yaar, D. Regev, S. Fredo, G. Shani, E. Arbaboff, W. Potzel, K. Aggarwal, J. A. Pereda, G. M. Kalvius, F. J. Litterst, W. Schäfer, and G. Will, Phys. Rev. B **42**, 8507 (1990).
[7] W. Suski, J. Magn. Magn. Mater. **90-91**, 99 (1990).
[8] A. V. Andreev, H. Nakotte, and F. R. de Boer, J. Alloys Compd. **182**, 55 (1992).
[9] K. Recko, M. Biernacka, L. Dobrzynski, K. Perzynska, D. Satua, K. Szymanski, J. Waliszewski, W. Suski, K. Wochowski, G. André, and F. Bourée, J. Phys.: Condens. Matter **9**, 9541 (1997).
[10] A. P. Gonçalves, P. Estrela, J. C. Waerenborgh, J. A. Paixão, M. Bonnet, J. C. Spirlet, M. Godinho, and M. Almeida, J. Magn. Magn. Mater. **189**, 283 (1998).
[11] A. P. Gonçalves, M. Almeida, C. T. Walker, J. Ray, and J. C. Spirlet, Mater. Lett. **19**, 13 (1994).
[12] M. Godinho, G. Bonfait, A. P. Gonçalves, M. Almeida, and J. C. Spirlet, J. Magn. Magn. Mater. **140-144**, 1417 (1995).
[13] G. Bonfait, M. Godinho, P. Estrela, A. P. Gonçalves, M. Almeida, and J. C. Spirlet, Phys. Rev. B **53**, R480 (1996); M. Godinho, P. Estrela, A. P. Gonçalves, M. Almeida, J. C. Spirlet, and G. Bonfait, J. Magn. Magn. Mater. **157-158**, 690 (1996).
[14] A. Paixão, B. Lebech, A. P. Gonçalves, P. J. Brown, G. H. Lander, P. Burlet, A. Delapalme, and J. C. Spirlet, Phys. Rev. B **55**, 14 370 (1997).
[15] J. C. Waerenborgh, A. P. Gonçalves, M. Godinho, and M. Almeida, J. Magn. Magn. Mater. **196-197**, 696 (1999).
[16] G. J. Long, T. E. Cranshaw, and G. Longworth, Moessbauer Eff. Ref. Data J. **6**, 42 (1983).
[17] J. C. Waerenborgh and F. Teixeira de Queiroz (unpublished).
[18] E.g., V. I. Goldanskii and E. F. Makarov, in *Chemical Applications of Mössbauer Spectroscopy*, edited by V. I. Goldanskii and R. H. Herber (Academic Press, New York, 1968), Chap. 1.